Bulletin of the New Zealand Society for Earthquake Engineering, Vol. 55, No. 4, December 2022

ESTIMATING FIRE FOLLOWING EARTHQUAKE RISK FOR WELLINGTON CITY, NEW ZEALAND

Finn Scheele[1], Biljana Lukovic[2], Jose Moratalla[3], Alexandre Dunant[4] and Nick Horspool[5]

(Submitted *September 2021*; Reviewed *December 2021*; Accepted *March 2022*)

ABSTRACT

Fire following earthquake (FFE) is a significant hazard in urban areas subject to high seismicity. Wellington City has many characteristics that make it susceptible to ignitions and fire spread. These include proximity to major active faults, closely spaced timber-clad buildings, vulnerable water and gas infrastructure, frequent high winds and challenging access for emergency services. We modelled the ignitions, fire spread and suppression for five earthquake sources. Uncertainty in ground motions, the number and location of ignitions, weather conditions and firefighting capacity were accounted for. The mean loss per burn zone (area burnt due to ignition and fire spread) is $46m without fire suppression, indicating the potential property damage avoided by controlling the fire spread. The mean total loss for earthquake scenarios ranges from $0.28b for the Wairau Fault through to $3.17b for a Hikurangi Subduction Zone scenario, including the influence of fire suppression. Wind speed has a strong influence on the potential losses for each simulation and is a more significant factor than the number of ignitions for evaluating losses. Areas in Wellington City of relatively high risk are identified, which may inform risk mitigation strategies. The models may be applied to other urban areas.

INTRODUCTION

Fires are common following earthquakes and occasionally develop into significant events with severe consequences. Earthquake damaged buildings and infrastructure lead to increased probabilities of ignition and fire spread, as electrical systems are damaged and fuel for burning is more readily available. Firefighting capacity and capability are often limited due to impaired road access and disrupted water supply.

Severe fire following earthquake (FFE) events are rare, with only a few major disasters resulting in widespread fire losses in the last few decades. Despite the rarity, FFE continues to be of concern due to the potential for significant losses that in some cases eclipse the impacts from the direct effects of earthquakes alone. One well known FFE event was the 1906 San Francisco earthquake, in which 28,000 buildings were destroyed across 12.2 km^2 of burnt area and approximately 3000 fatalities were reported, due to both the earthquake and fire [1]. An even larger event was the 1923 Great Kantō earthquake which destroyed an estimated 447,000 houses across 38.3 km^2 of burnt area and resulted in 140,000 fatalities. An investigation by Himoto [2] of damaging earthquakes in Japan between 1995 and 2017 found that ignitions were associated with 14 out of 24 events (58%). Of these, the most severe impacts were from the 1995 Kobe earthquake, in which there were 293 ignitions and 7288 buildings destroyed by fire, and the 2011 Tōhoku earthquake and tsunami which resulted in 330 ignitions, although fire damage was mainly constrained to buildings and materials already substantially damaged by ground shaking or tsunami effects. In the US, ignitions were associated with several Californian earthquakes between 1971 and 2000, most notably the 1994 Northridge earthquake which resulted in approximately 110 ignitions, although most fires were constrained to the structure of origin [1]. New Zealand's only major FFE event occurred following the 1931 Napier earthquake, in which fire destroyed much of the central business district [3,4].

Wellington City has many characteristics that make it susceptible to FFE. Wellington is located in a zone of high seismic hazard, has geography which may enhance fire spread and pose difficulties for access, is frequently windy, has many closely spaced timber-clad buildings and has vulnerable infrastructure including gas and water mains. To better understand the risk and impacts of FFE in Wellington City we have modelled ignitions and fire spread for ground shaking produced by several potential earthquake sources and accounted for wind conditions and suppression due to firefighting activities. This article also includes a brief review of FFE models available globally. The study area for FFE modelling is the urban area of Wellington City, as shown in Figure 1. For modelling and reporting purposes, Statistical Area 2 (SA2) are used, defined by Stats NZ as areas that reflect communities that interact together socially and economically, similar to suburbs, as shown in Figure 2.

BACKGROUND TO FFE IGNITION AND FIRE SPREAD MODELLING

We reviewed the literature on FFE focusing on the various ignition, fire spread and fire suppression models that are available. Lee et al. [5] provide a comprehensive review of models up until the date of publication, and therefore we focused primarily on literature published subsequently. This section provides a brief summary of the review, which is described in more detail in Scheele and Horspool [6].

[1] *Corresponding Author, Risk Scientist, GNS Science, Lower Hutt, f.scheele@gns.cri,nz*
[2] *Senior GIS Analyst / Modeller, GNS Science, Lower Hutt*
[3] *Risk Engineer, GNS Science, Lower Hutt*
[4] *Postdoctoral Research Associate, Durham University, Durham*
[5] *Natural Hazard Risk Scientist, GNS Science, Lower Hutt*

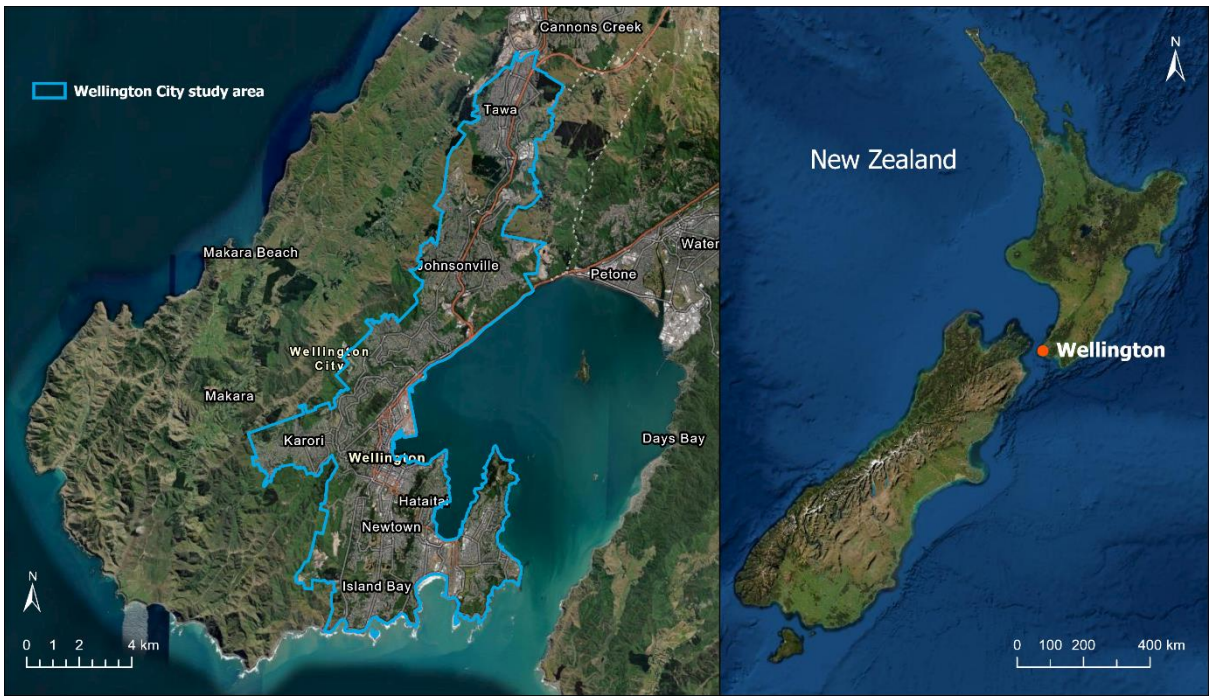

Figure 1: Wellington City study area and location within New Zealand.

Ignition

Ignitions following earthquakes are most commonly caused by damage to electrical or gas supply systems, including mains breaks and overturning of appliances [1]. For example, in the 1994 Northridge, United States earthquake there were 110 ignitions of which 54 were related to gas system failures [7]. Gas is a fuel source, with the actual ignition most often caused by electrical network failures. Ignitions are commonly associated with the immediate impacts of an earthquake, however there may be ignitions occurring in the subsequent days following the main shake. Himoto [2] found a similar pattern between two major earthquake events in Japan (1995 Kobe and 2011 Tōhoku earthquakes), in which approximately 70% of ignitions occurred within the first 24 hours and the remaining 30% were spread across the following 9 days. Ignitions across a 21-day period following the 2011 Tōhoku earthquake were evaluated by Nishino and Hokugo [8], showing a similar pattern as found by Himoto [2] with the ignition rate dropping to normal levels beyond about 10 days. The time-dependency of ignitions is an important factor for estimating suppression via firefighting because of changes in the capacity of emergency services. Although there have been many earthquake events accompanied by ignitions globally, the limited number of FFE events that have involved significant fire spread in Japan and the US form the basis of most empirical data and studies on the phenomenon.

Lee et al. [5] reviewed FFE ignition models and found that the majority are regression models that relate the frequency of ignition with a measure of ground motion intensity, such as peak ground acceleration (PGA) or Modified Mercalli Intensity (MMI). The response variable (output) is usually the number of ignitions per a unit of building floor area (such as millions of square feet). Lee et al. [5] noted that there is a high level of uncertainty in the source data, due a lack of information about how the data were collected and analysed.

More recent ignition models include a range of covariates to more accurately estimate ignition probability based on the characteristics of an area or the earthquake event, such as population density or the collapse ratio of buildings, in addition to measures of ground motion intensity. Examples include studies by Davidson [9] and Anderson et al. [10], where statistically FFE ignitions were modelled using generalised linear and generalised linear mixed models, based on US and Japanese event data respectively.

For this study, we used ignition equations developed by Elhami Khorasani et al. [11] based on historical data from seven US earthquake events (1983–2014). The probability of ignition can be estimated for both census tracts (a US statistical geography similar to SA2) and individual buildings. Within census tracts, probability of ignition is based on peak ground acceleration, building square area and population density. For individual buildings, the construction type is an additional factor. The application of the ignition model is described in the section on ignition modelling.

Fire Spread

Post-earthquake fire spread models estimate the area burnt, considering the characteristics of the built environment and the ignition locations. Recent FFE models are mostly simulations, many of which utilise GIS and physics-based fire spread equations. Models may incorporate various factors, for example building attributes (combustibility, building separation, height), weather (wind speed and direction, rain), vegetation, slope, fire suppression, and so on. Empirical data underpins models to various degrees, with most observations from events in Japan and the United States.

The earliest FFE spread model was developed by Hamada [12]. The built environment is represented by equally-spaced blocks of buildings, and fire spreads in an elliptical shape. The Hamada model is based on a series of empirically-derived equations, incorporating wind speed and direction, building footprint dimensions, building separation distance and a factor of how built-up the area is. Several subsequent models (e.g. HAZUS; [13]) adopt the same basic approach as the Hamada model, while altering the equations used. The Cousins et al. static model [14,15] is a further example of this approach, using buffers around building footprints to define potential burn-zones, simulating the critical separation distance a fire may spread between buildings given physical rules and wind speed. Locations of ignitions are randomly assigned to estimate building and monetary losses from those burn-zones. All buildings within a burn-zone are assumed to be a total loss if an ignition is present. The static model was applied to Wellington City as a probabilistic tool for estimating post-earthquake fire losses.

Figure 2: Wellington City suburbs represented by SA2s.

The 2000s saw a number of models developed which took advantage of improvements in computational power, data availability and spatial analysis software. Cellular automata is a frequently employed technique, in which an area is divided into grid cells that are assigned properties and states depending on the time step. For example, a cell's properties determine how combustible it is, and the state is whether it is burning (and if so, the intensity). Physics-based rules determine whether fire will spread to the next cell. At each time step, all cells are scanned to determine their state. Examples include the Cousins et al. dynamic model [14,16-18]. The Cousins et al. dynamic model was developed for estimating fire spread in the New Zealand context as a real-time firefighting tool.

Multiple models were created that incorporate the physics of fire spread more directly, including radiation, convection, temperature, piloted ignition, branding and fire impedance [5]. The ResQ Firesimulator [19] models fire spread using heat transport methods (radiation, convection, direct transport) as well as a grid which simulates wind. Individual buildings are modelled, and include attributes of building combustibility, separation distance, and contents. Iwami et al. [20] simulate fire spread based on heat development over time within a burning building, with spread occurring to a nearby building if it reaches a critical temperature or flames touch. Building factors for this model include combustibility, openings, and contents; wind speed and direction is also accounted for. Himoto and Tanaka [21] simulate urban fire spread per building considering three physical factors: thermal radiation, wind-blown fire plumes, and firebrand spotting.

Recently developed models have attempted to comprehensively simulate FFE. Zhao [22] developed the GisFFE model, which uses physical properties and rules to estimate both fire development within a single building following an ignition, as well as fire spread between buildings (via thermal radiation, thermal plume heating and firebrand spotting). Factors include temperature, humidity, rain and wind. Nishino et al. [23] incorporate the same factors of fire spread as Zhao [22], as well as wind speed and direction, and air temperature. Additionally, fire spread is assessed in two stages, both within a building and spreading to other buildings, using physics-based rules at each stage. The Urban Fire Simulation (UFS) model [24,25] similarly includes a module to estimate fire development within a building, considering fire spread from room-to-room based on compartment fire literature. Algorithms are used to estimate room configuration where layout is unknown. Fire spread to other buildings is from either exterior rooms (via flame impingement, window flame radiation, gas radiation or vegetation), or from roofs (via flame radiation or branding). The UFS model is probabilistic, with the results of multiple runs able to be combined to show the relative risk per building within the simulated area. Existing fire spread models generally do not account for the contribution of severe building damage, where the exposed combustible interiors and contents aid fire spread.

Suppression

The effect of suppression on ignitions and fire spread is an important part of estimating losses and forms the basis for evaluating most mitigation strategies. Suppression is performed either by emergency services or residents and community members. Key considerations for emergency services are firefighting capacity, response time, road access and water availability [1,26].

Li and Davidson [25] conducted a parametric study of the factors that influence fire spread and developed a firefighting module for their fire spread simulator based on expert elicitation with US fire department personnel and review of previous models [24]. They concluded that availability of water for firefighting has the strongest influence on the number of buildings burnt, with arrival time of fire engines also having an influence. These factors are in addition to the scenario factors of number of ignitions and wind speed. The firefighting module simulates multiple activities at each time step: the list of fires is updated; reported fires are given a priority based on building area; engine needs for each fire are calculated; the status of each engine is updated; water is applied to a fire based on the rate of each engine's contribution; and finally spread potential is modified. A similar approach was taken by Zhao [22] where firefighting activities are considered in five steps: fire discovery; fire report; fire response; arrival of fire brigade; and fire control. HAZUS [27] incorporates fire suppression by factoring multiple activity steps, namely discovery time, report time, arrival time, control time, and mop-up time.

The effect of fire suppression by residents was modelled by Nishino et al. [23] and Himoto and Tanaka [28]. Using data from the 1995 Kobe earthquake, Nishino et al. [23] estimated that the probability of an ignition being suppressed by residents is 0.204 and reduced the number of ignitions that lead to fire spread in their modelling accordingly. Himoto and Tanaka [28] assessed the ability of residents to fight fires by considering external factors (e.g. range of burning buildings relative to the location of fire hydrants, dangers of approaching target buildings) and human factors of decision-making, given the environmental situation. The latter model was designed to measure the effect of residents fighting involved fires rather than suppressing ignitions.

Recent studies by Li et al. [29] and Davis et al. [26] highlight the importance of the water distribution network for firefighting. Li et al. [29] developed a model to assess water infrastructure performance for post-earthquake firefighting, simulating pipe damage and hydraulic performance over time. Davis et al. [26] modelled ignitions and water demand for firefighting across five earthquake scenarios affecting Los Angeles, estimating the water flow required to suppress fires in each scenario, and concluded that a rapid response is essential.

Suppression was accounted for in previous modelling for Wellington City as described in Cousins et al. [15]. The study used Modified Mercalli Intensity (MMI) as an indication of overall earthquake intensity for the Wellington Fault. Up to MMI 8, mains water and access was assumed to be available and emergency services could control ten post-earthquake fires, with a linear decrease in firefighting capacity up to MMI 11, where zero fires are suppressed resulting in total loss.

EARTHQUAKE SCENARIOS

To understand the range of impacts from FFE, five earthquake scenarios presenting a significant seismic hazard for Wellington City were chosen for ground motion simulation. These are earthquakes on the Wellington Hutt Valley fault segment (WellWHV), the Wairau Fault, the Wairarapa Fault and two scenarios on the Hikurangi Subduction Margin Interface (HikWgtnMax and HikWgtnMin). The fault sources and characteristics are taken from the National Seismic Hazard Model (NSHM) [30]. The magnitude (M_W), length, depth, rake and return period of these fault sources are summarised in Table 1. The mean peak ground accelerations (PGA) across Wellington City's statistical geographic areas (SA2s) are shown in Table 2. The approximate location of the fault sources is shown in Figure 3, mapped as the top edge of the rupture used in the ground motion modelling, along with the hypocentre (the point where an earthquake rupture starts). The hypocentre is assumed to always be on the top edge of the earthquake rupture for all the cases considered here.

The Wellington Hutt Valley fault segment is the largest contributing source of seismic hazard for Wellington for PGAs above 0.3 g [31] and has an approximate 10% chance of rupturing within the next 100 years [32] with an earthquake

around magnitude 7.5. The Wairau Fault is part of the Marlborough Fault System in the northern part of the South Island, extending offshore towards Wellington. It may be nearing the end of its interseismic period [33]. The earthquake on the Wairau Fault is chosen as a smaller scenario relative to the other fault sources with regards to expected PGAs for Wellington City. The Wairarapa Fault is simulated based on the source characteristics of the 1855 earthquake and causes a similar level of ground shaking to the Wellington Fault scenario when averaged across all SA2s. The Hikurangi Subduction Margin source is represented by HikWgtnMax and HikWgtnMin, which are two possible rupture locations of different magnitude and proximity to Wellington. The fault sources and associated earthquake scenarios from the NSHM are simplified representations of reality.

Table 1: Fault sources and characteristics for simulation of ground motions.

Fault Source	Mag. (Mw)	Length (km)	Depth (km)	Rake (°)	Return Period (Years)
WellWHV	7.5	73	0	0	830
Wairau	7.8	144	0	0	1150–1400
Wairarapa	8.2	156	0	0	1200
HikWgtnMax	8.6	224	5	90	1100
HikWgtnMin	8.2	219	15	90	600

Ground motions were simulated using the OpenQuake software [34]. Primary inputs include the fault characteristics (Table 1), sites of interest exposed (in this case, the Wellington SA2s) and the local site conditions (e.g. rock or soil, which affects local seismic amplification, obtained from a Vs30 map). Each SA2 was assessed for ground motions individually, with the Vs30 values averaged across the area of each SA2. The averaging was necessary to obtain areal PGA values required by the ignition equations described in the section on ignition modelling. Various ground motion prediction equations (GMPEs) were used, depending on the fault source characteristics (e.g. active shallow crust or subduction interface). There is a large amount of variability regarding the ground motions at any given site for a given earthquake source and magnitude. To account for this, ground motions are simulated for each SA2 thousands of times (15,000 for WellWHV, Wairau and Wairarapa and 3,000 for HikWgtnMax and HikWgtnMin). Ground motions were output as PGA in units of g (acceleration due to Earth's gravity).

Due to the computational power required to run the fire spread model, it was necessary to select particular percentiles that represent the distribution of PGAs for each earthquake source. These were chosen as the median value and three percentiles above and below the median, i.e. 0.001, 0.02, 0.16, 0.5, 0.84, 0.98 and 0.999 percentiles. Note that, as described in the ignition modelling section, the PGA values for the 0.999 percentile are very high for most sources and lead to an unrealistic number of ignitions estimated by the ignition model. Further, GMPEs usually give extreme results at large percentiles, because they are no longer constrained by empirical data. Therefore, the 0.999 percentile is removed from model runs and reporting, as well as the 0.001 percentile to maintain an even distribution (unless otherwise explicitly mentioned).

The mean PGAs and ranges across all Wellington SA2s for each fault source and percentile shown in Table 2 describe the different ground motions experienced. WellWHV and Wairarapa have similar mean and ranges across all percentiles. HikWgtnMin and HikWgtnMax have similar mean values as WellWHV and Wairarapa up to the 50th percentile, but significantly increased PGAs at the higher percentiles and also a large range across the SA2s. The Wairau fault source has the lowest PGAs, only high enough to generate significant numbers of ignitions at the 98th percentile (see Table 3).

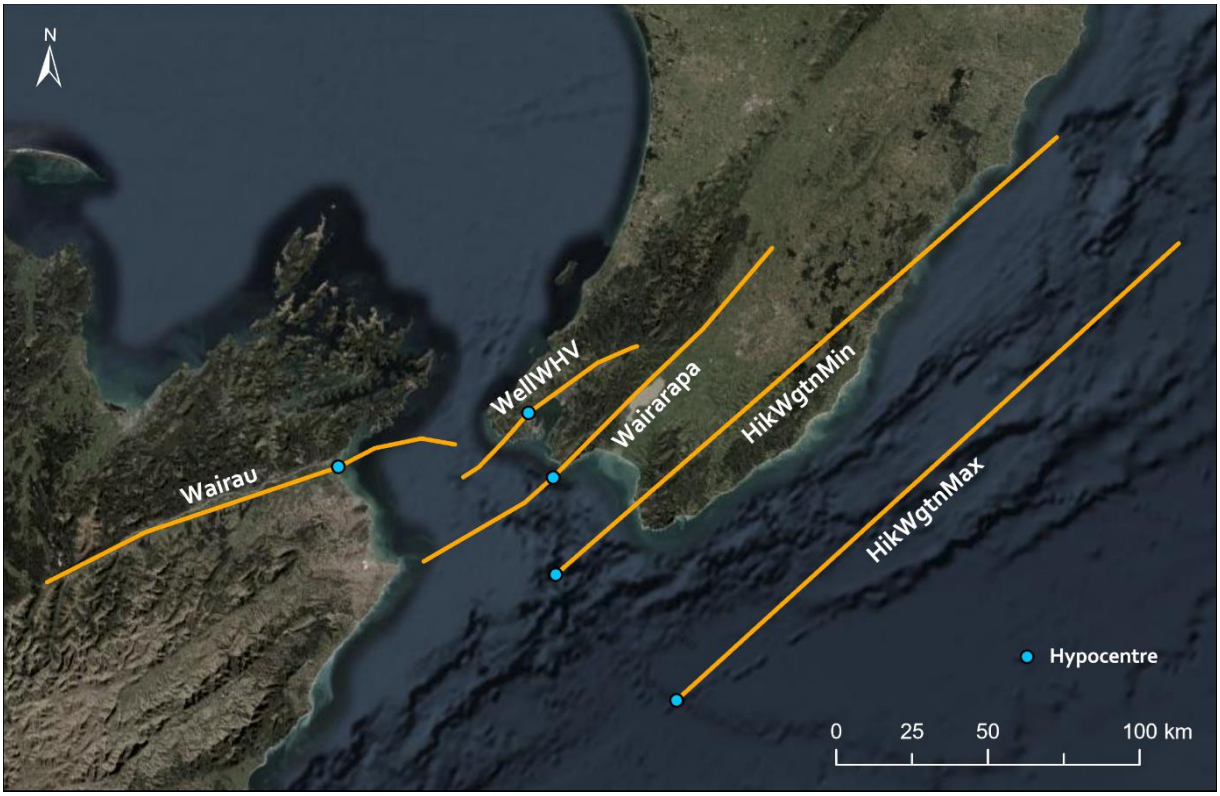

Figure 3: The top edge and hypocentre of each fault source, giving an approximate location of earthquake source as modelled. The locations may differ in real events.

Table 2: Fault sources and mean PGA across all Wellington City SA2s for each percentile. The PGA values in brackets are the minimum and maximum values across all SA2s for each percentile.

Fault Source	Mean PGA (g) for Wellington City SA2s				
	2nd Percentile	16th Percentile	50th Percentile	84th Percentile	98th Percentile
WellWHV	**0.14** (0.1–0.18)	**0.26** (0.19–0.34)	**0.46** (0.34–0.62)	**0.83** (0.56–1.07)	**1.52** (0.91–2.01)
Wairau	**0.05** (0.03–0.08)	**0.1** (0.06–0.14)	**0.17** (0.12–0.23)	**0.31** (0.22–0.41)	**0.58** (0.41–0.79)
Wairarapa	**0.13** (0.09–0.19)	**0.25** (0.17–0.35)	**0.46** (0.34–0.61)	**0.85** (0.5 –1.12)	**1.6** (0.95–2.09)
HikWgtnMax	**0.11** (0.08–0.13)	**0.24** (0.16–0.27)	**0.49** (0.36–0.55)	**1.03** (0.74–1.17)	**2.21** (1.54–2.54)
HikWgtnMin	**0.1** (0.07–0.12)	**0.22** (0.16–0.26)	**0.47** (0.35–0.52)	**0.97** (0.72–1.11)	**2.09** (1.5 – 2.44)

Table 3: Mean number of ignitions for each fault source and percentile. Numbers in brackets are the minimum and maximum values.

Fault Source	All Percentiles	2nd Percentile	16th Percentile	50th Percentile	84th Percentile	98th Percentile
WellWHV	**126** (0–574)	**1** (0–4)	**2** (0–6)	**11** (5–18)	**105** (85–130)	**512** (455–574)
Wairau	**6** (0–39)	**0** (0–2)	**1** (0–3)	**1** (0–4)	**3** (0–10)	**26** (12–39)
Wairarapa	**139** (0–630)	**0** (0–4)	**2** (0–6)	**10** (1–19)	**116** (81–146)	**569** (506–630)
HikWgtnMax	**235** (0–1016)	**1** (0–3)	**1** (0–4)	**12** (5–19)	**208** (168–234)	**952** (880–1016)
HikWgtnMin	**212** (0–940)	**1** (0–3)	**1** (0–7)	**10** (3–18)	**178** (155–219)	**873** (745–940)

IGNITION AND FIRE SPREAD MODELLING FOR WELLINGTON CITY

Ignition and fire spread modelling were run for 100 simulations of each earthquake source and percentile ground motion, totalling 500 simulations between the 2nd and 98th percentile for each fault source. The 0.001 percentile was also run for all fault sources, but only reported where explicitly mentioned. The 0.999 percentile was not run due to unrealistic numbers of ignitions and prohibitive computational requirements. Additionally, 3,000 simulations of WellWHV at the 50th percentile were run to evaluate the uncertainty of ignition locations and wind speed and direction (see Section 0). The modelling development was first described in a pair of reports by Scheele et al. [35,36].

Ignition Modelling

The ignition model used for this study was developed by Elhami Khorasani et al. [11]. The model is appropriate for Wellington City because of the ability to estimate the probability of ignition for individual buildings and the required building attribute data is available. The method for applying the ignition model follows.

The ignition model requires inputs of PGA, total building floor square footage (SF), population density (PD), and building construction (wood, non-combustible or mobile home). Non-combustible buildings refer to the structural system, such as concrete, masonry or steel [11]. PGA is obtained from ground motion simulations as described in Section 0. SF and building construction are from a building database maintained by GNS Science and the National Institute of Water and Atmospheric Research (NIWA) and population is from the 2018 New Zealand census data.

First, the probability of ignition is estimated for SA2s. The PGA values for each SA2 are attached for each fault source and percentile, and total SF and PD are also calculated for each SA2. Once the probability of ignition is obtained for SA2s, the probability is applied to individual buildings within each SA2. In the original model [11], the number of buildings of each construction type is used to spread ignition probability between individual buildings within an area unit. However, because there are very few mobile homes in the study area and because the probability of ignition is very similar for wood and non-combustible buildings in the ignition model, all buildings are treated equally. In part, this is also to account for the uncertainty regarding building attributes, particularly because the external cladding attribute is often unreliable in the available database. The number of buildings in each SA2 is calculated using the number of building footprint centroids that fall inside the boundaries of each SA2. The probability of

ignition for each building is then applied using the equations described in Elhami Khorasani et al. [11].

For estimating whether an ignition occurs in a building, a random number between 0 and 1 is generated. If the generated number is less than the probability of ignition, the building is considered to be ignited, and if the number is higher, it is not. Each simulation run generates different numbers and distributions of ignitions. The mean number of ignitions for each fault source and percentile is summarised in Table 3. The mean number of ignitions per SA2 is plotted against PGA in Figure 4.

Applying the ignition model to Wellington City has some caveats. The size of the area for calculating probability of ignition matters. In previous work [36], the equations were tested using meshblocks (the smallest geographical subdivision for produced by Stats NZ); however, unrealistically high probabilities of ignition were produced. This is likely because the empirical source data used to derive the equations is at the scale of US census tracts (a statistical subdivision with a population between 1,200 and 8,000 people), which are bigger than meshblocks. Therefore, SA2s were used here because they are similar in size to census tracts.

Elhami Khorasani et al. [11] note that, at higher shaking intensities, PGA has a much greater effect than SF or PD (especially for PGAs greater than 0.6 g). This effect is demonstrated by the plot in Figure 4. Notably, the empirical ignition data from US events were mostly for PGAs less than 0.6 g, whereas, in the higher percentiles of the scenarios in this study, PGAs may exceed 2 g (Table 2). For the highest percentile (0.999), the number of ignitions was excessive, reaching more than 27,000 ignitions for HikWgtnMax with a mean PGA of 4.7 g. This is unrealistic and represents a very extreme scenario resulting in total loss for essentially all of Wellington City. Therefore, the 0.999 percentile was removed from modelling. The 98th percentile also has a very high number of ignitions and sufficiently represents extreme scenarios.

Compared to the ignition model developed by Cousins et al. [14], the overall mean number of ignitions is similar. This is expected, if the models have been applied correctly, because both models were developed using datasets of FFE ignitions from US events (in many cases, the same data).

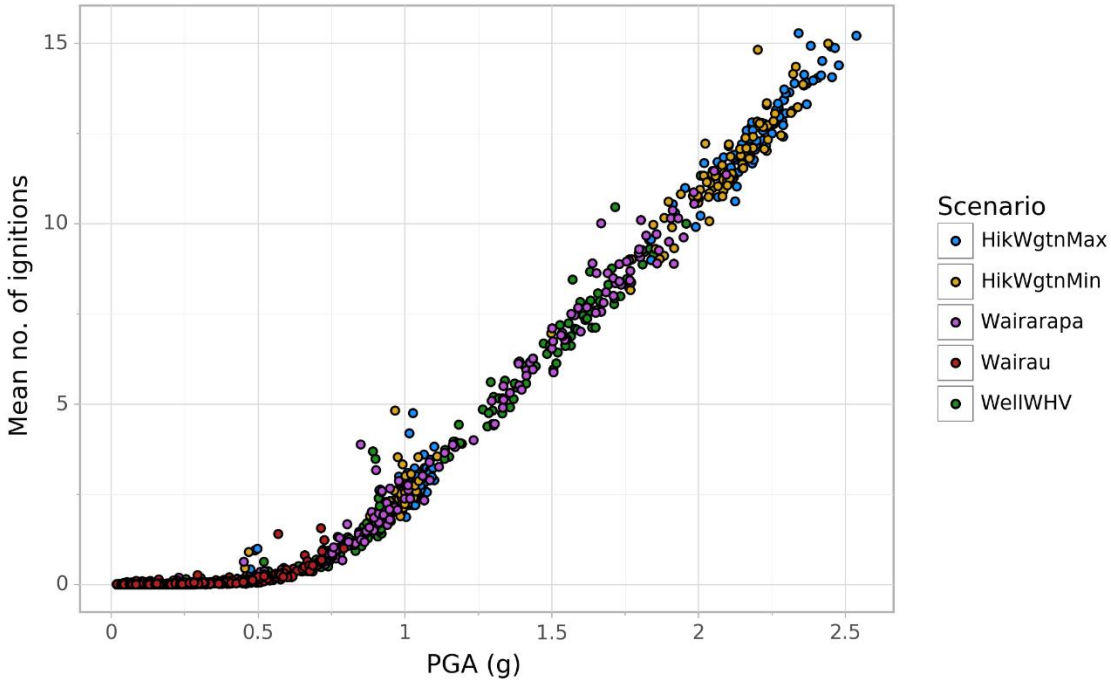

Figure 4: Mean number of ignitions per SA2 against PGA. The lowest percentile (0.001) is also included in this plot.

Fire Spread Modelling

The new fire spread model developed for Wellington City is conceptually based on the static burn zone model by Cousins et al. [14]. Attributes from the building database, represented as points, were spatially matched to building footprints obtained from Land Information New Zealand. Buffers around building footprints are used to account for the maximum distance that fire will spread to another building, based on the critical separation distance (dependent on wind speed) as shown in Table 4. The critical separation distances signify the maximum distance a fire can spread given the wind conditions and rules to account for physical fire behaviour such as direct contact, heat radiation and branding. The values were derived from loss and wind speed data as reported from historical US earthquakes by Scawthorn [37], and the method is described in Thomas et al. [16].

The most important difference in the current spread modelling is the inclusion of wind direction information, which alters how buffers around buildings are applied. Unlike the static burn zone model, in which burn zones are pre-calculated depending on the critical separation distance (effectively dividing the built environment into blocks), the spread model we developed is calculated on the fly.

The ‘construction type’ attribute from the building database was used to determine whether a building is combustible or not. All wooden buildings are combustible, and all other types are assumed to be non-combustible. Fire is assumed not to spread to non-combustible buildings but, if an ignition starts in one, the building is assumed to burn but fire will not spread from there. This assumption reflects the potential for ignitions to start in any building, causing damage and loss internally even if the building construction is generally non-combustible.

To estimate fire spread, first the ignition model is used to distribute ignitions across buildings within the study area. From wind rose data based on a decade of observations for Wellington City, wind speed and direction are randomly selected based on the probability of each wind speed and

direction occurring. Ignited combustible buildings are then buffered by the critical separation distance for calm conditions (12 m). Depending on the wind conditions, the buffer is then moved in the direction of the wind until the critical separation distance for that wind speed is reached. Any building that falls within the buffers and is combustible will catch fire, and the buffering process on newly ignited buildings will begin until the critical separation distance is reached. This process continues until no further buildings are ignited, i.e. the fire has spread as far as it can, given the conditions. The resulting burn zones can vary in size considerably, as shown in the mapped simulation run in Figure 5.

By using moving buffers of 12 m separation distance, the assumption that fire can spread in all directions due to physical processes (such as radiation) is maintained, as well as incorporating the effects of wind speed and direction. This is a significant improvement over the static model Cousins et al. [14], which assumes that fire can spread evenly in all directions based on the wind speed (critical separation distance) but does not account for wind direction. In the static model, burn zones can become unreasonably large for higher wind speeds.

Table 4: Wind speed and critical separation distance (the maximum distance a fire can spread, given the wind conditions), derived from historical US earthquake data (adapted from Cousins et al. [14]; data originally from Scawthorn [37])

Wind Speed (km/h)	Critical Separation Distance (m)
0–4.9 (calm)	12
5–9.9	13
10–14.9	13
15–19.9	14
20–24.9	16
25–29.9	18
30–34.9	23
35–39.9	28
40–44.9	33
45–49.9	42
50+	45

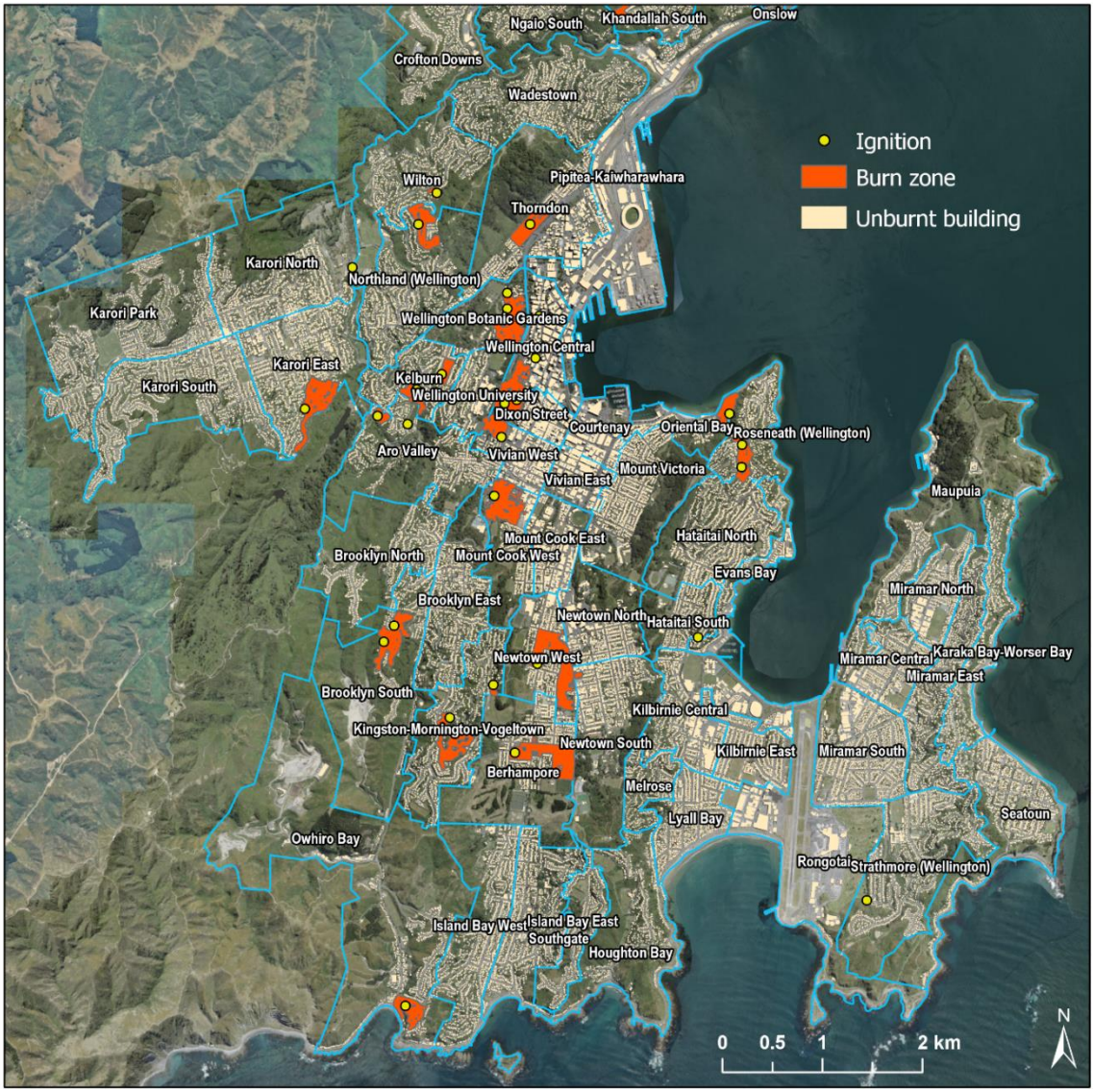

Figure 5: Example of ignition locations and fire spread for one simulation run of the WellWHV scenario at the 50th percentile. Every simulation run of the model will produce different ignition distributions and burn zone extents.

To generate loss and impact information, the final burn zone buffers are dissolved (joined together) and all building footprints that are within the burn zones are used to calculate loss (building replacement value) and other impacts (e.g. population affected). Note that loss estimates are just the maximum possible fire loss, as the existing shaking loss or losses from other perils that might damage a building before fire breaks out, such as tsunami, are not calculated first.

Suppression Modelling

Suppression is accounted for in the current loss modelling by considering the conditions of each scenario and the potential response. The factors included are the number of ignitions, ignition suppression by residents, firefighting capacity over time and availability of mains water and road access. The approach uses the statistical summaries for each scenario (i.e. each fault source and percentile) and does not have an explicit spatial component (e.g. via GIS). The assumptions and justifications are provided as follows.

For assessing availability of mains water and road access, the median PGA across all SA2s for each scenario is used as a proxy for estimating disruption. Where median PGA is less than 0.2 g, water and access are assumed to be available for firefighting. Between 0.2 and 0.5 g, access is variable, with some ignitions unable to be reached, and water is unavailable. Where median PGA is greater than 0.5 g, water is unavailable and access is increasingly limited. The value of 0.2 g for water supply disruption is based on previous work modelling water outage due to earthquakes in the New Zealand context described in Uma et al. [38], where damage and outage to the water supply network is expected at this value of PGA. Assumptions regarding access are loosely based on the potential for building collapse and landslides, given PGA.

Ignitions are divided across ten days, following the observation from earthquakes in Japan [2] that 70% of ignitions occur within the first day and the remainder are relatively evenly distributed across the following nine days. Twenty percent of ignitions are suppressed by residents, using the value provided by Nishino et al. [23], and therefore the loss estimates before evaluating the effect of firefighting by emergency services are also reduced by 20%. The firefighting capacity of emergency services in Wellington City is assumed to be ten ignitions per day, as per Cousins et al. [15]. Total loss is assumed for ignitions that are not addressed by residents or emergency services, i.e. when the number of ignitions is greater than ten for any given day (after the 20% reduction by resident suppression).

Suppression via firefighting by emergency services and the associated reduction in loss is based on the conditions as follows. Where water and access are available, fires are mostly suppressed with only some building damage (10% loss). Where water is unavailable and access is variable, half of the building damage is mitigated (50% loss). Where water is unavailable and access is limited, only 20% of the building damage is mitigated (80% loss).

The assumptions within the suppression model are intended to reflect the magnitude of each scenario and account for the limited resources for firefighting. The resulting reduction in losses is substantial for smaller magnitude scenarios, whereas more extreme scenarios with many ignitions will overwhelm the capacity of emergency services. Further work on development of the suppression model should incorporate feedback by emergency services on capacity, given scenarios of varying magnitude, and should include specific spatial analysis of water supply infrastructure and road access.

SCENARIO MODELLING RESULTS

This section describes the results of running 100 simulations of the ignition and spread models for each fault source and percentile, totalling 500 simulations between the 2nd and 98th percentile for each fault source. Losses accounting for suppression are summarised in Table 5. WellWHV and Wairarapa show very similar losses across all percentiles at $2.04b and $2.24b, respectively, which is expected because of the similar PGAs. HikWgtnMax and HikWgtnMin are also similar, representing the highest losses across the scenarios, at $3.17b and $3.01b, respectively. Wairau shows the lowest losses, at $0.28b. Notably, across all fault sources and percentiles there is a large range of losses between simulation runs.

The losses without suppression are provided for comparison in Table 6. Across all percentiles, suppression accounts for the greatest difference across for the WellWHV and Wairau scenarios, with a reduction in loss of 37% and 42% respectively. The Wairarapa, HikWgtnMax and HikWgtnMin scenarios all have a similar reduction of 26%, 24% and 25% respectively. Regardless of scenario, suppression accounts for the greatest reduction in loss in percentiles where the firefighting capacity of emergency services is not overwhelmed.

Table 5: Mean loss from fire (billions of dollars) for each fault source and percentile including suppression (bolded). The minimum and maximum loss for each percentile is in brackets.

Fault Source	All Percentiles	2nd Percentile	16th Percentile	50th Percentile	84th Percentile	98th Percentile
WellWHV	**2.04** (0–14.28)	**0** (0–0.07)	**0.04** (0–0.95)	**0.26** (0.01–1.34)	**2.8** (1.27–10.98)	**7.08** (5.0–14.28)
Wairau	**0.28** (0–6.21)	**0** (0–0.17)	**0.01** (0–0.15)	**0.01** (0–0.15)	**0.12** (0–2.01)	**1.28** (0.17–6.21)
Wairarapa	**2.24** (0–15.1)	**0** (0–0.04)	**0.07** (0–0.75)	**0.25** (0.01–1.43)	**3.03** (1.21–10.93)	**7.83** (5.04–15.1)
HikWgtnMax	**3.17** (0–16.99)	**0.01** (0–0.13)	**0.05** (0–0.67)	**0.45** (0.04–2.49)	**4.74** (2.33–13.22)	**10.6** (7.57–16.99)
HikWgtnMin	**3.01** (0–16.75)	**0** (0–0.11)	**0.04** (0–0.51)	**0.3** (0.01–2.01)	**4.5** (2.08–12.69)	**10.22** (7.35–16.75)

Table 6: Mean loss from fire (billions of dollars) for each fault source and percentile without suppression (bolded). The minimum and maximum loss for each percentile is in brackets.

Fault Source	All Percentiles	2nd Percentile	16th Percentile	50th Percentile	84th Percentile	98th Percentile
WellWHV	**2.79** (0.0–18.78)	**0.06** (0.0–0.84)	**0.1** (0.0–2.37)	**0.7** (0.03–4.07)	**3.82** (1.73–14.95)	**9.3** (6.58–18.78)
Wairau	**0.48** (0.0–9.33)	**0.05** (0.0–2.12)	**0.06** (0.0–1.85)	**0.09** (0.0–1.9)	**0.31** (0.0–5.03)	**1.91** (0.25–9.33)
Wairarapa	**3.04** (0.0–19.79)	**0.04** (0.0–0.5)	**0.17** (0.0–1.88)	**0.66** (0.01–3.68)	**4.12** (1.64–14.82)	**10.24** (6.62–19.79)
HikWgtnMax	**4.18** (0.0–21.82)	**0.07** (0.0–1.66)	**0.12** (0.0–1.67)	**0.71** (0.07–3.89)	**6.38** (3.14–17.79)	**13.61** (9.74–21.82)
HikWgtnMin	**4.03** (0.0–21.56)	**0.04** (0.0–1.37)	**0.1** (0.0–1.27)	**0.77** (0.03–6.11)	**6.07** (2.8–17.13)	**13.15** (9.5–21.56)

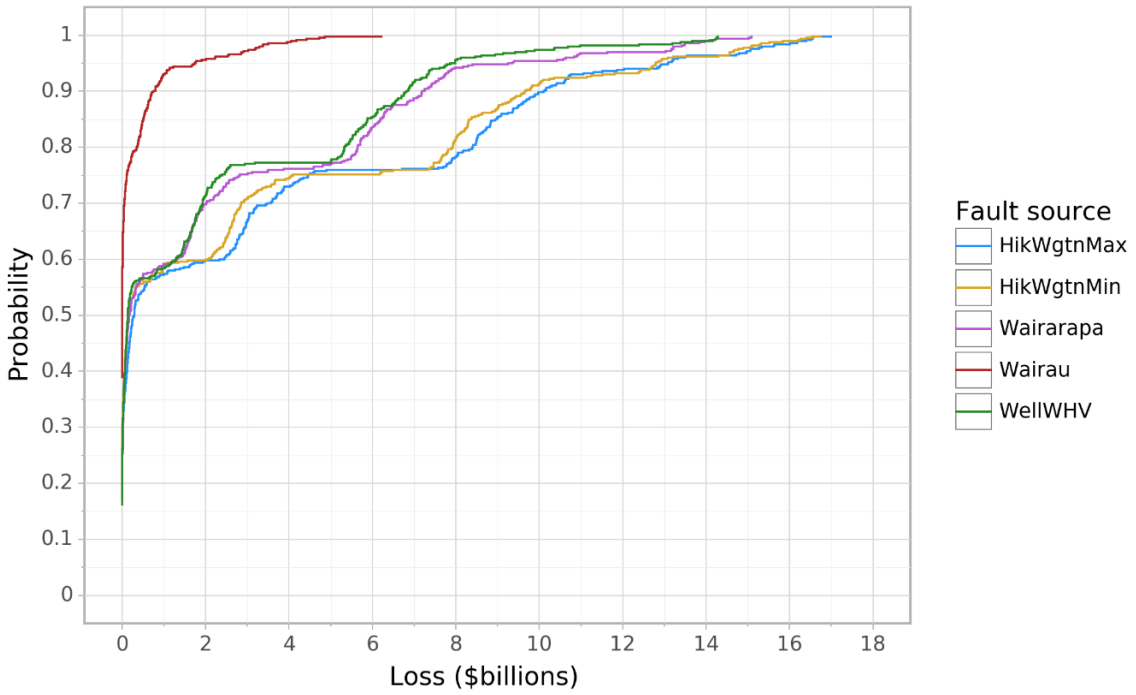

Figure 6: Cumulative distribution function showing probability of loss being equal or less than a given value for each fault source, given an event.

The probability that loss will be equal or less than a given value for each fault source is shown by the cumulative distribution function in Figure 6. As an example, there is about a 90% probability of loss being less than $7b for the WellWHV and Wairarapa scenarios and about a 90% probability of loss being less than $10b for HikWgtnMax and HikWgtnMin scenarios.

The graph in Figure 7 lists the twenty suburbs with the highest mean loss ratio (the loss divided by the replacement value of buildings) across all scenarios, without suppression. The frequency of loss per meshblock is mapped in Figure 8, calculated as the number of buildings burned in a meshblock (summed for all scenarios) divided by the number of buildings in the meshblock (to normalise for meshblock size). The map shows the areas of Wellington that are at relatively high or low risk from FFE. Hataitai, Newtown and the fringe suburbs around the CBD experience the most frequent modelled loss, due to relatively high population densities and closely spaced combustible buildings. The map displays risk at a finer resolution than the graph, which is based on SA2s, and some suburbs will have areas of higher and lower risk, altering the ranking. Note that suppression is not included in the calculations for the graph or map because of the way the modelling results were analysed. Not including suppression has little influence on relative risk, but the mean loss ratios in Figure 7 would be lower if suppression was included.

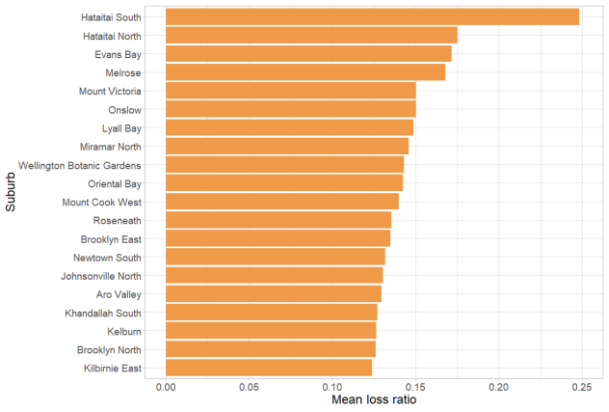

Figure 7: The twenty suburbs with the highest mean loss ratio across all scenarios without fire suppression.

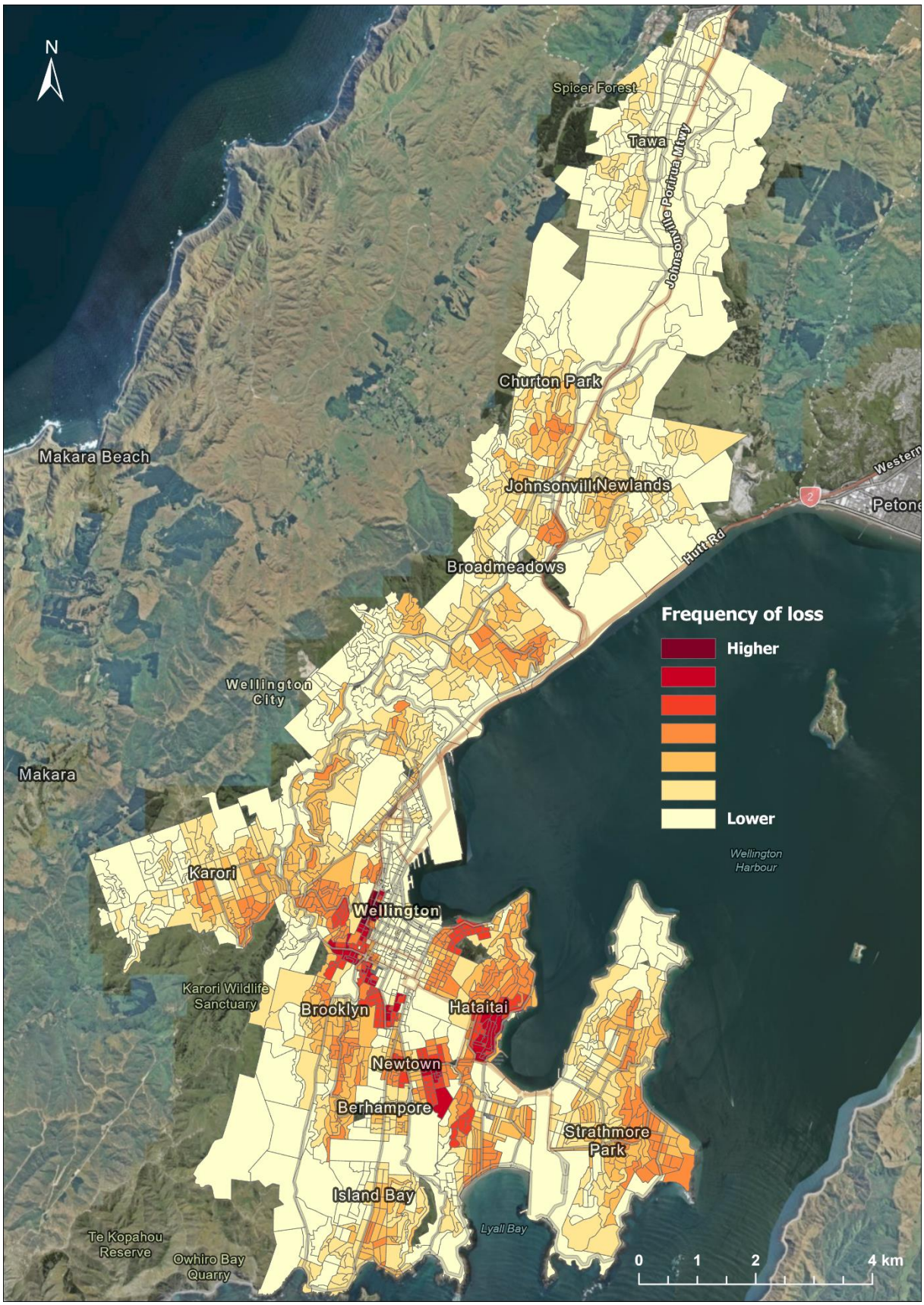

Figure 8: The frequency of loss per meshblock without fire suppression, calculated as the number of buildings burned in a meshblock (summed for all scenarios) divided by the number of buildings in a meshblock (to normalise for meshblock size).

The distribution of loss per individual burn zone (without suppression) is shown in Figure 9, showing a reasonably lognormal distribution. The median loss per burn zone is $18.5m, and the mean loss is $46m. The usually-resident (night) population per burn zone is shown in Figure 10, which has a similar lognormal distribution. The median number of people per burn zone is 132, and the mean is 324. The loss and population values per burn zone give an indication of the potential impact from extinguishing an ignition before fire spreads.

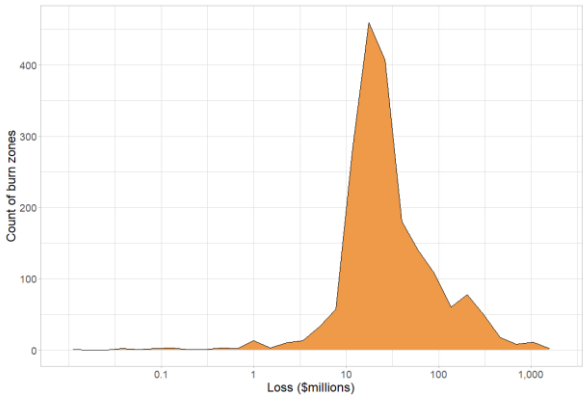

Figure 9: The distribution of loss per burn zone (in millions of dollars). The mean loss per burn zone is $46m.

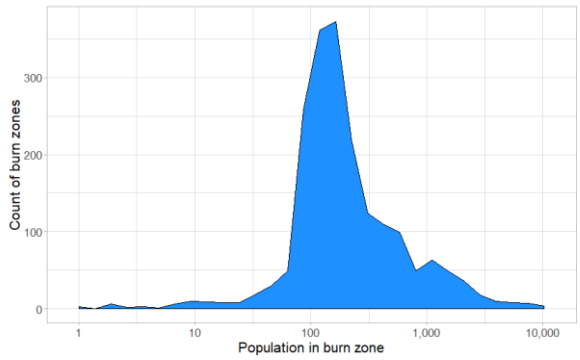

Figure 10: The distribution of population per burn zone, with a mean of 324 people.

The simulation run variables of wind speed, and number of ignitions are examined against loss to identify potential relationships. Losses are similar for all wind speeds up until about 20 km/h (Figure 11), reflecting the very modest increases in critical separation distances (Table 4). For wind speeds over about 25 km/h, there is an increase in loss of about $1b for every 10 km/h wind speed increase up to 50 km/h, although there is also increasing spread in loss values. The relationship is less clear over 50 km/h wind speeds, which may be due to the far fewer data points available compared to lower wind speeds, as only about 3% of simulation runs had wind speeds over 50 km/h. North-west and south/south-east winds dominate the higher losses because of high maximum wind speeds.

The relationship between number of ignitions, loss and wind speed is plotted in Figure 12. Higher losses are clearly associated with higher wind speeds. The number of ignitions also has an influence, contributing to higher losses, although with a less pronounced effect as wind speed.

To test the number of simulation runs required to give stable loss results, given the uncertainty across input variables (known as convergence), 3,000 simulation runs of WellWHV at the 50th percentile were performed. The results are graphed using the cumulative mean loss per simulation run without suppression in Figure 13. Every simulation run for a given fault source and percentile contains random sampling to determine the number and distribution of ignitions and the wind speed and direction. Convergence is reached when there are enough simulation runs that doing additional runs does not change the results significantly. Figure 13 shows good stability in loss results from about 1,300 simulation runs. A reasonable approximation of the mean loss is established between 100–200 simulation runs.

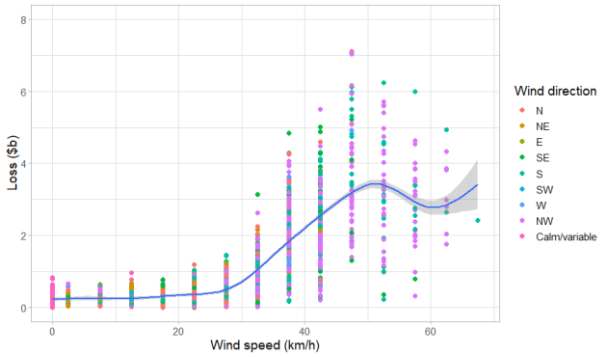

Figure 11: Relationship between wind speed (km/h) and loss (billions of dollars, without suppression) for all simulation runs.

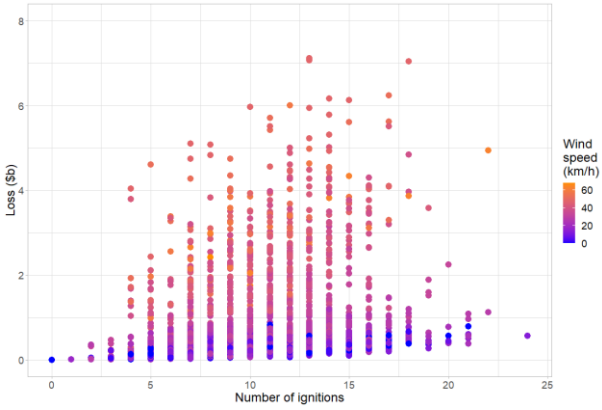

Figure 12: Relationship between number of ignitions and loss (billions of dollars, without suppression) for all simulation runs.

Figure 13: Cumulative mean loss without suppression for 3,000 simulation runs of WellWHV at the 50th percentile.

The relationship between loss ratio for SA2s and PGA is displayed in Figure 14. There is an increasing trend of loss ratio, most strongly observed from about 0.5 g, in line with the mean number of ignitions plotted against PGA in Figure 4. A cumulative distribution function was fitted to the data with an estimated mean of 2.41 and standard deviation of 0.93. From this relationship, it was possible to produce a rough estimate of loss for areas where the ground motions have been modelled and a building database is available.

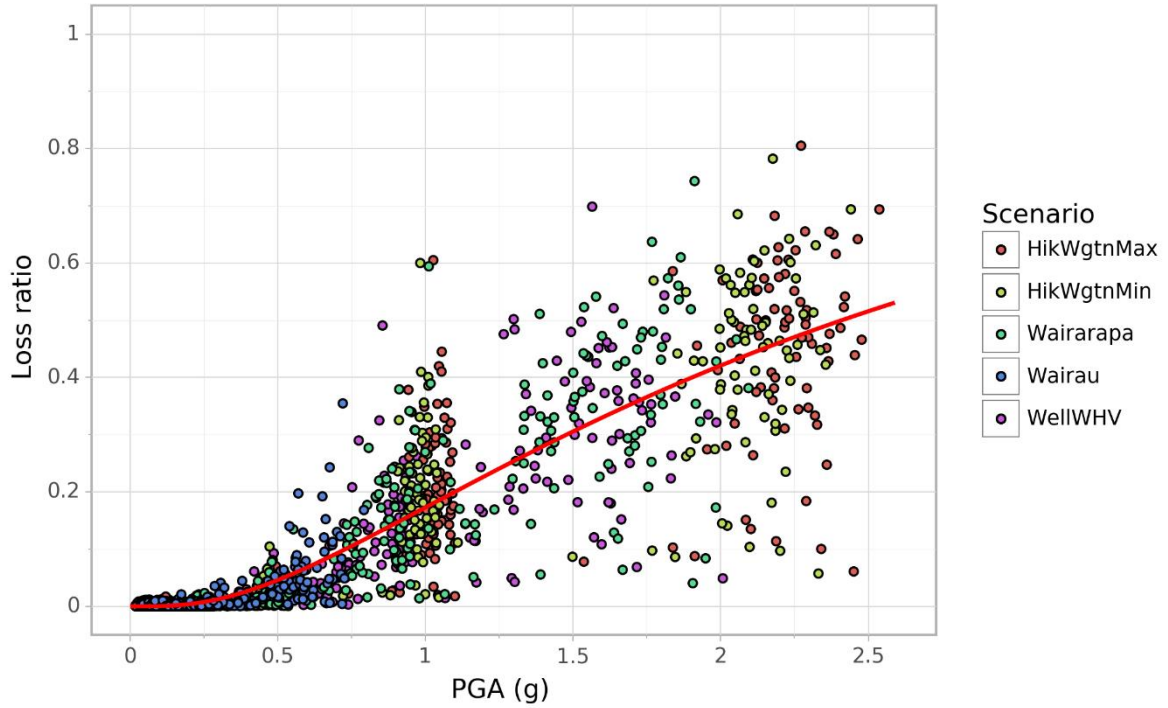

Figure 14: Loss ratio against PGA (g) for SA2s and all fault sources.

Loss was estimated for Lower Hutt, Upper Hutt and Porirua cities using the cumulative distribution function (Table 7). Ground motions for the same fault sources and percentiles for Wellington City were simulated using the OpenQuake software for all Greater Wellington SA2s. The RiskScape building database was used to aggregate the building replacement cost per SA2. Therefore, the loss estimates are the result of the relationship between PGA, the replacement cost and the loss ratio. The advantage of this technique is that the ignition and spread models do not need to be run for the new areas of interest. However, the loss estimates are highly uncertain and the required data for further analysis, such as suppression and mapping, are not produced.

The assumptions are that the urban environments of Lower Hutt, Upper Hutt and Porirua are similar to Wellington City on average (e.g. building types and separation distances) and that the wind rose data for Wellington City reasonably reflects the overall wind conditions in Greater Wellington. The loss estimates in Table 7 should only be considered as a rough order of magnitude estimate for each fault source affecting Greater Wellington. Wellington and Lower Hutt cities experience greater losses than Upper Hutt or Porirua cities from the fault sources in this study.

Table 7: Mean loss (billions of dollars) for cities in Greater Wellington for the 50th percentile of each fault source (without suppression).

Scenario	Wellington City	Lower Hutt City	Upper Hutt City	Porirua City	Total
WellWHV	0.7	0.53	0.11	0.12	1.46
Wairau	0.09	0.02	0.01	0.01	0.13
Wairarapa	0.66	0.82	0.29	0.15	1.92
HikWgtnMax	0.71	0.73	0.22	0.35	2.01
HikWgtnMin	0.77	0.65	0.2	0.31	1.93

DISCUSSION

The ignition and spread modelling for Wellington City accounts for multiple earthquake sources and variability in ground motions, number and locations of ignitions, and variation in wind speed and direction. The suppression model improves the loss estimates by accounting for firefighting by residents and emergency services, firefighting capacity over time, and disruption to mains water and road access. The combination of these models allows identification of areas of relatively high risk, which is useful for the targeting of risk mitigation strategies. There are uncertainties and limitations within the modelling, which are discussed here.

Variability in ground motions is accounted for by sampling the distributions of PGA using percentiles for each fault source. Due to computational limitations, only five percentiles were chosen, whereas it would be desirable to have more to fully account for the distribution of PGAs. Additionally, the number and distribution of ignitions and wind speed and direction are sampled using random numbers for each simulation run. As there are only 100 simulations per percentile, the distribution of possible scenarios will not be fully accounted for. Wind speed and direction is assumed to be constant for the duration of a simulation run, whereas, in reality, conditions are likely to change across the duration of an event.

The building database utilised for the ignition model and fire spread contains a reasonable representation of building footprints across Wellington City, but the attributes of the buildings such as the cladding and construction type are of varying quality. Further work to improve the building database would also improve the ignition and fire spread modelling, particularly with regard to combustibility.

The ignition model used [11] has some caveats. Firstly, the model only estimates the potential ignitions in buildings. Ignitions and potential fire spread from other sources are not considered in the modelling. For example, broken gas pipelines are a potential ignition and fuel source that are not explicitly accounted for. Secondly, the ignition model predicts very large numbers of ignitions at higher PGAs, which are likely to be an

overestimation. This is partly due to the maximum PGAs of the source data to be around 0.6 g, whereas the GMPEs used within this study predict PGAs in excess of this value for the higher percentiles of most earthquake scenarios. Therefore, the resulting loss estimations for the higher percentiles (84th and 98th) may be significant overestimations and should be treated with caution. Thirdly, recent earthquakes in New Zealand produced significant PGAs in urban areas (e.g. the 2010-2011 Canterbury earthquake sequence and the 2016 Kaikōura earthquake) yet resulted in few ignitions (two in separate Canterbury earthquakes). Running the ignition model for these scenarios would produce many ignitions. Further research should be undertaken to understand the reasons for so few ignitions and the implications for applying ignition models to New Zealand urban areas developed using data from overseas events.

For practical reasons, it is necessary to simplify the modelling of physical processes that lead to ignition and fire spread. The fire spread model and critical separation distances were developed with respect to physical rules, but do not explicitly consider all modes of fire spread independently. Depending on the scenario, specific processes (e.g. branding) may have significant effects that are not fully accounted for in the modelling. Two notable factors for fire spread are slope and vegetation, which are not currently incorporated in the spread model. Including slope would require development of a 3D model, whereas the current model assumes a flat topography. Vegetation could be included in the current spread model, if data on the distribution and combustibility of vegetation was available at an appropriate resolution. Currently available data is too coarse for this purpose. Fire spread through severely damaged buildings is an additional factor not accounted for in this study, or commonly included in existing published models. The combustible interior and contents of buildings may be exposed due to damage and could be a significant factor for fire spread.

The processing time of the fire spread simulations is currently very slow, with a single run potentially taking many hours when there are large numbers of ignitions and strong wind conditions, using a high specification desktop computer. Readily applying the spread model to other urban areas would be aided by the use of high performance computing and further investigation into optimisation techniques.

The suppression model developed for this study incorporates a number of assumptions regarding firefighting resources and simplifies the estimation of water availability and road access based on PGA values. Wellington has several challenges that influence the ability to address fires in a post-earthquake scenario, such as potential landslides affecting road access, that require detailed and bespoke methods to address in modelling. Other suppression models that are published for overseas contexts are a useful guide but are not readily applicable to Wellington City, due to differences in access, water supply networks, and firefighting capacity.

For any given simulation run, the distribution of ignitions and fire spread will be different from a real event. While examination of individual simulation runs (e.g. Figure 5) can be useful for understanding possible outcomes of FFE events, the results are better interpreted once aggregated or analysed considering many simulation runs. Additionally, pre-existing loss from earthquake shaking or other perils is not currently accounted for but could be in the future (as it was for shaking in Cousins et al. [15]).

Applying models to Wellington City that are developed using empirical data from international historical events assumes that the characteristics of the events and the local context are similar. Although fire spread characteristics are the same, building construction and sources of ignition differ between locations. The difference is difficult to quantify without extensive research.

Finally, validation is a problem for all FFE modelling due to relatively few events having occurred in recent decades. The original fire spread models that this study are based upon have been validated against the 1931 Napier and 1995 Kobe events with good results [16]. However, the required data for validation of the models used in the current study were not readily available. Future work should include validation where possible.

CONCLUSIONS

The potential for ignition and fire spread was modelled for Wellington City to identify areas of relatively high risk and the losses for various earthquake scenarios. Five earthquake sources representing major faults near the study area were selected. Through literature review we selected an appropriate ignition model for application to Wellington developed by Elhami Khorasani et al. [11]. Fire spread modelling between buildings is based on physical rules and is adjusted based on the wind speed and direction for each simulation run. Each scenario was run hundreds of times to account for uncertainty in ground motions, number and locations of ignitions, and weather conditions. Suppression by residents and emergency services is accounted for based on the number of ignitions and estimates of disruption to water mains and road access. The models are transferable to other urban areas of New Zealand.

Across all scenarios, the mean loss for burn zones (the extent of fire spread from an ignition) is $46m, indicating the potential savings of suppressing an ignition. The mean population within burn zones is 324. Wind speed is shown to have a very strong effect on the loss estimates, and the number of ignitions also has an influence. By considering the weather conditions following an earthquake event, a rapid assessment of the threat from FFE could be undertaken.

The results of this study are most useful for identifying the areas of relative FFE risk across Wellington City, and as a relative comparison of the impact between earthquake scenarios. The relative risk identification may be used to inform the targeted implementation of risk mitigation strategies. The loss results are conservative, especially for the higher percentiles of ground motions, where the ignition model is likely overpredicting the number of ignitions. Further research should be undertaken to examine the applicability to urban areas of New Zealand of models developed using empirical data from overseas events. Examining the reasons for the low number of ignitions in recent local earthquakes compared to ignition model predictions would assist in improving the understanding of FFE risk in New Zealand.

Future work should also focus on the development of the suppression model to better account for emergency service response, for example by using network modelling to account for access disruption. The influence of risk mitigation strategies should also be incorporated into suppression modelling, which can be used as an evidence base for addressing the problem of FFE in urban areas.

ACKNOWLEDGMENTS

The authors would like to thank Fire and Emergency New Zealand, the Wellington Region Emergency Management Office, Wellington Lifelines Group, Wellington Water and Wellington City Council for their input into the FFE modelling process. We are grateful for funding from It's Our Fault for this study. We appreciate the constructive comments from reviewers of this article.

REFERENCES

1. Scawthorn C, Eidinger JM and Schiff A (2005). "*Fire Following Earthquake"*. ISBN: 978-0-7844-0739-4, American Society of Civil Engineers (ASCE), Reston, 332 pp.
2. Himoto K (2019). "Comparative analysis of post-earthquake fires in Japan from 1995 to 2017". *Fire Technology*, **55**(3): 935–961. https://doi.org/10.1007/s10694-018-00813-5
3. Dowrick DJ (1998). "Damage and intensities in the magnitude 7.8 1931 Hawke's Bay, New Zealand, earthquake". *Bulletin of the New Zealand Society for Earthquake Engineering*, **31**(3): 139–163. https://doi.org/10.5459/bnzsee.31.3.139-163
4. Heron D, Cousins J, Thomas G, Lukovic B and Schmid R (2003). "*Fire-Following Earthquake – Napier 1931 Revisited"*. Consultancy Report 2003/95, GNS Science, Lower Hutt, 32 pp.
5. Lee S, Davidson R, Ohnishi N and Scawthorn C (2008). "Fire following earthquake – Reviewing the state-of-the-art of modelling". *Earthquake Spectra*, **24**(4): 933–967. https://doi.org/10.1193/1.2977493
6. Scheele F and Horspool N (2018). "*Modelling Fire Following Earthquake in Wellington: A Review of Globally Available Methodologies*". Science Report 2017/42, GNS Science, Lower Hutt, 23 pp. http://dx.doi.org/10.21420/G27S7V
7. California Seismic Safety Commission (2002). "*Improving Natural Gas Safety in Earthquakes*". SSC-02-03, ASCE-25 Task Committee on Earthquake Safety Issues for Gas Systems, West Sacramento, 49 pp. https://ssc.ca.gov/wp-content/uploads/sites/9/2020/08/cssc_2002-03_natural_gas_safety.pdf
8. Nishino T and Hokugo A (2020). "A stochastic model for time series prediction of the number of post-earthquake fire ignitions in buildings based on the ignition record for the 2011 Tohoku Earthquake". *Earthquake Spectra*, **36**(1): 232–249. https://doi.org/10.1177/8755293019878184
9. Davidson RA (2009). "*Generalized Linear (Mixed) Models of Post-Earthquake Ignitions"*. Technical Report MCEER-09-0004, Multidisciplinary Center for Earthquake Engineering Research (MCEER), Buffalo, 110 pp. https://www.eng.buffalo.edu/mceer-reports/09/09-0004.pdf
10. Anderson D, Davidson RA, Himoto K and Scawthorn C (2016). "Statistical modeling of fire occurrence using data from the Tōhoku, Japan earthquake and tsunami". *Risk Analysis*, **36**(2): 378–395. https://doi.org/10.1111/risa.12455
11. Elhami Khorasani N, Gernay T and Garlock M (2017). "Data-driven probabilistic post-earthquake fire ignition model for a community". *Fire Safety Journal*, **94**: 33–44. https://doi.org/10.1016/j.firesaf.2017.09.005
12. Hamada M (1951). *On fire spreading velocity in disasters*. Sagami Shobo, Tokyo.
13. Sasaki K and Sekizawa A (2014). "Risk assessment of fire spread potential for a densely built-up area using a simulation model of fire spread and fire-fighting". *Bulletin of Japan Association for Fire Science and Engineering*, **64**(3), 29–37. https://doi.org/10.11196/kasai.64.3_29
14. Cousins J, Thomas G, Heron D, Mazzoni S and Lloydd D (2002). "*Estimating Risks from Fire Following Earthquake*". Client Report 2002/60, Institute of Geological & Nuclear Sciences, Lower Hutt, 43 pp.
15. Cousins J, Thomas G, Heron D and Smith W (2012). "Probabilistic modeling of post-earthquake fire in Wellington, New Zealand". *Earthquake Spectra*, **28**(2): 553–571. https://doi.org/10.1193/1.4000002
16. Thomas G, Heron D, Cousins J and de Róiste M (2012). "Modeling and estimating post-earthquake fire spread". *Earthquake Spectra*, **28**(2): 795–810. https://doi.org/10.1193/1.4000009
17. Ohgai A, Gohnai Y, Ikaruga S, Murakami M and Watanabe K (2004). "Cellular automata modeling for fire spreading as a tool to aid community-based planning for disaster mitigation". Page 193–209 in Recent Advances in Design and Decision Support Systems in Architecture and Urban Planning. Editors: Van Leeuwen JP and Timmermans HJP, ISBN: 978-1-4020-2408-5, Kluwer, Dordrecht.
18. Olsen E and Morgante A. *Modeling Fire following Earthquake for the 2013 Japan Model Update*. Verisk. http://www.air-worldwide.com/Publications/AIR-Currents/2013/Modeling-Fire-Following-Earthquake-for-the-2013-Japan-Model-Update/ (Accessed 28 March 2022)
19. Nüssle TA, Kleiner A and Brenner M (2004). "*Approaching urban disaster reality: The resQ firesimulator"*. Page 474-482 in *RoboCup 2004: Robot Soccer World Cup VIII*. Editors: Nardi D, Riedmilelr M, Sammut C and Santos-Victor J, ISBN: 978-3-540-32256-6, Springer, Germany.
20. Iwami T, Ohmiya Y, Hayashi Y, Kagiya K, Takahashi W and Naruse T (2004). "Simulation of city fire". *Fire Science and Technology*, **23**(2): 132–140. https://doi.org/10.3210/fst.23.132
21. Himoto K and Tanaka T (2008). "Development and validation of a physics-based urban fire spread model". *Fire Safety Journal*, **43**(7): 477–494. https://doi.org/10.1016/j.firesaf.2007.12.008
22. Zhao S (2010). "GisFFE—An integrated software system for the dynamic simulation of fires following an earthquake based on GIS". *Fire Safety Journal*, **45**(2): 83–97. https://doi.org/10.1016/j.firesaf.2009.11.001
23. Nishino T, Tanaka T and Hokugo A (2012). "An evaluation method for the urban post-earthquake fire risk considering multiple scenarios of fire spread and evacuation". *Fire Safety Journal*, **54**: 167–180. https://doi.org/10.1016/j.firesaf.2012.06.002
24. Li S and Davidson R (2013). "Application of an urban fire simulation model". *Earthquake Spectra*, **29**(4): 1369–1389. https://doi.org/10.1193/050311EQS111M
25. Li S and Davidson RA (2013). "Parametric study of urban fire spread using an urban fire simulation model with fire department suppression". *Fire Safety Journal*, **61**, 217–225. https://doi.org/10.1016/j.firesaf.2013.09.017
26. Davis C, Scawthorn C, Coles C and Abustan L (2019). "Fire following earthquake risk assessment: the city of Los Angeles' efforts toward water system seismic resilience and sustainability". *International Conference on Sustainable Infrastructure 2019: Leading Resilient Communities through the 21st Century*, November 6–9, Los Angeles, California, 12 pp. https://doi.org/10.1061/9780784482650.058
27. Federal Emergency Management Agency (2009). *Hazus-MH 2.1 Technical Manual – Earthquake Model*. https://www.fema.gov/sites/default/files/2020-09/fema_hazus_earthquake-model_technical-manual_2.1.pdf
28. Himoto K and Tanaka T (2012). "A model for the fire-fighting activity of local residents in urban fires". *Fire Safety Journal*, **54**: 154–166. https://doi.org/10.1016/j.firesaf.2012.04.006

29. Li Y, Gao J, Zhang H, Deng L and Xin P (2019). "Reliability assessment model of water distribution networks against fire following earthquake (FFE)". *Water*, **11**(12): 2536. https://doi.org/10.3390/w11122536
30. Stirling, M, McVerry G, Gerstenberger M, Litchfield N, Van Dissen R, Berryman K., Barnes P, Wallace L, Villamor P and Langridge R (2012). "National seismic hazard model for New Zealand: 2010 update". *Bulletin of the Seismological Society of America*, **102**(4): 1514–1542. https://doi.org/10.1785/0120110170
31. Smith WD and Harmsen SC (2010). "Displaying seismic deaggregation: the importance of the various sources". *Seismological Research Letters*, **81**(3): 488–497. https://doi.org/10.1785/gssrl.81.3.488
32. Rhoades D, Van Dissen R, Langridge R, Little T, Ninis D, Smith E and Robinson R (2011). "Re-evaluation of conditional probability of rupture of the Wellington-Hutt Valley segment of the Wellington Fault". *Bulletin of the New Zealand Society for Earthquake Engineering*, **44**(2): 77–86. https://doi.org/10.5459/bnzsee.44.2.77-86
33. Zachariasen J, Berryman K, Langridge R, Prentice C, Rymer M, Stirling M and Villamor P (2006). "Timing of late Holocene surface rupture of the Wairau Fault, Marlborough, New Zealand". *New Zealand Journal of Geology and Geophysics*, **49**(1): 159–174. https://doi.org/10.1080/00288306.2006.9515156
34. Pagani M., Monelli D, Weatherill G, Danciu L, Crowley H, Silva V, Henshaw P, Butler L, Nastasi M and Panzeri L (2014). "OpenQuake engine: An open hazard (and risk) software for the global earthquake model". *Seismological Research Letters*, **85**(3): 692–702. https://doi.org/10.1785/0220130087
35. Scheele F, Lukovic B, Moratalla J, Dunant A and Horspool N (2020). "*Modelling Fire Following Earthquake for Multiple Scenarios Affecting Wellington City"*. Science Report 2020/12, GNS Science, Lower Hutt, 26 pp. https://doi.org/10.21420/H7PX-XD46
36. Scheele F, Lukovic B and Horspool N (2019). "*Revisiting Fire Following Earthquake Modelling for Wellington City".* Science Report 2019/24, GNS Science, Lower Hutt, 27 pp. https://doi.org/10.21420/QYQ1-RE79
37. Scawthorn C (1987). "Fire Following Earthquake: Estimates of the Conflagration Risk to Insured Property in Greater Los Angeles and San Francisco". All Industry Research Advisory Council.
38. Uma SR, Scheele F, Abbott E and Moratalla J (2021). "Planning for resilience of water networks under earthquake hazard". *Bulletin of the New Zealand Society for Earthquake Engineering*, **54**(2): 135–152. https://doi.org/10.5459/bnzsee.54.2.135-152